6. miniworkshop difrakce a ultraperiferálních srážek

Notes on writing a paper for ALICE

Guillermo Contreras

Czech Technical University in Prague

Děčín

September 14, 2023

6. miniworkshop difrakce a ultraperiferálních srážek

This is not a guide nor a 'bible'!
The goal is to help you to find your own style

Notes on writing a paper for ALICE

Guillermo Contreras

Czech Technical University in Prague

Děčín
September 14, 2023

Questions to be addressed

What have we done?

Questions to be addressed

Why have we done it?

What have we done?

Questions to be addressed

Why have we done it?

What have we done?

How have we done it?

Questions to be addressed

Why have we done it?

What have we done?

How have we done it?

What did we find?

Questions to be addressed

Why have we done it?

Precise description of what you have done.

What have we done?

How have we done it?

What did we find?

Questions to be addressed

Why have we done it?

What is the physics you want to address? what are the open questions in the field? what other work has been done in the past to address these questions? What new knowledge is expected from this work and why?

Precise description of what you have done.

What have we done?

How have we done it?

What did we find?

Questions to be addressed

Why have we done it?

What is the physics you want to address? what are the open questions in the field? what other work has been done in the past to address these questions? What new knowledge is expected from this work and why?

Precise description of what you have done.

What have we done?

How have we done it?

What did we find?

This should be the 'easy' part: here you describe your work. The amount of detail depends on the journal, if there are other papers to refer to, if there is something new in the methods ...

Questions to be addressed

Why have we done it?

What is the physics you want to address? what are the open questions in the field? what other work has been done in the past to address these questions? What new knowledge is expected from this work and why?

What have we done?

Precise description of what you have done.

How have we done it?

This should be the 'easy' part: here you describe your work. The amount of detail depends on the journal, if there are other papers to refer to, if there is something new in the methods ...

What did we find?

Compare your work to expectations and discuss the findings: do they correspond to expectations or not and why.

Structure of an article

Structure of an article

Use it to answer either what was done or what was found

Short (~12 words), assertive, factual

Title

Structure of an article

Title

Abstract

Short (~12 words), assertive, factual

Use it to answer either what was done or what was found

Keep it short (~5 to 8 sentences). Write a first version before starting the paper, then a new version after you have finished the paper.

It should contain what you did and what you found.

Structure of an article

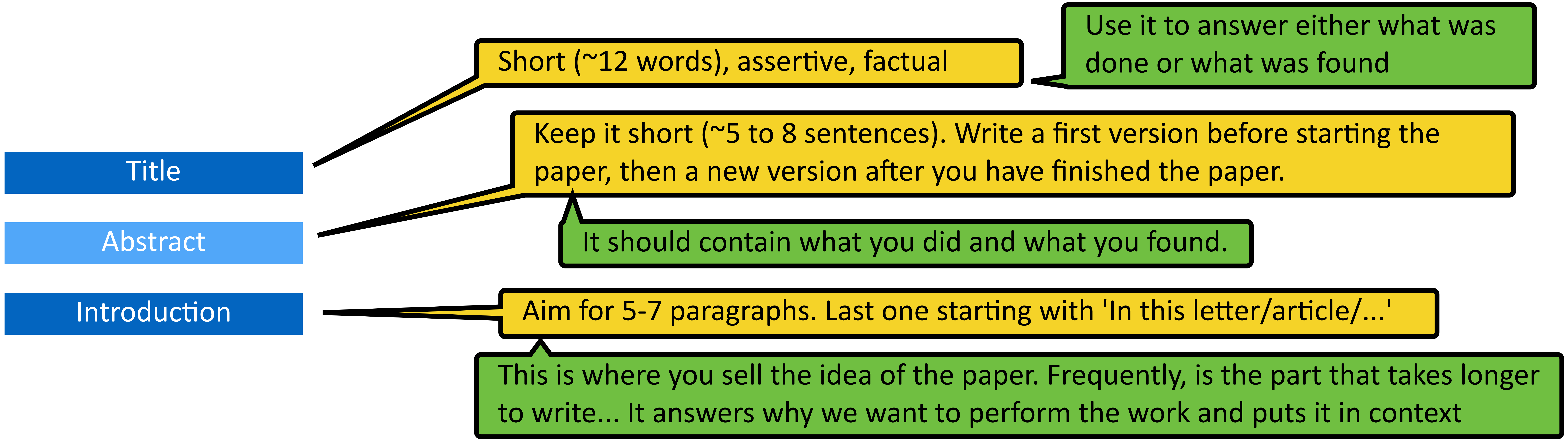

Structure of an article

Title

Short (~12 words), assertive, factual

Use it to answer either what was done or what was found

Abstract

Keep it short (~5 to 8 sentences). Write a first version before starting the paper, then a new version after you have finished the paper.

It should contain what you did and what you found.

Introduction

Aim for 5-7 paragraphs. Last one starting with 'In this letter/article/...'

This is where you sell the idea of the paper. Frequently, is the part that takes longer to write... It answers why we want to perform the work and puts it in context

Experimental set up

Analysis

As long as necessary, but not longer ...

This is your work. It has to be clear and complete.

Structure of an article

Short (~12 words), assertive, factual

Use it to answer either what was done or what was found

Keep it short (~5 to 8 sentences). Write a first version before starting the paper, then a new version after you have finished the paper.

It should contain what you did and what you found.

Aim for 5-7 paragraphs. Last one starting with 'In this letter/article/...'

This is where you sell the idea of the paper. Frequently, is the part that takes longer to write... It answers why we want to perform the work and puts it in context

As long as necessary, but not longer ...

This is your work. It has to be clear and complete.

Keep it short and factual

Make sure the results can be used even if our understanding of the issues at hand changes: include tables with as many numbers as possible ...

- Title
- Abstract
- Introduction
- Experimental set up
- Analysis
- Results

Structure of an article

Title

Abstract

Introduction

Experimental set up

Analysis

Results

Discussion

Short (~12 words), assertive, factual

Use it to answer either what was done or what was found

Keep it short (~5 to 8 sentences). Write a first version before starting the paper, then a new version after you have finished the paper.

It should contain what you did and what you found.

Aim for 5-7 paragraphs. Last one starting with 'In this letter/article/...'

This is where you sell the idea of the paper. Frequently, is the part that takes longer to write... It answers why we want to perform the work and puts it in context

As long as necessary, but not longer ...

This is your work. It has to be clear and complete.

Keep it short and factual

Make sure the results can be used even if our understanding of the issues at hand changes: include tables with as many numbers as possible ...

As long as necessary, but not longer ...

Compare to expectations and models in a clear and factual way. Enumerate all caveats in the comparison. Based on this, conclude on what we learn and how we could proceed for the next steps.

Structure of an article

- Title
  - Short (~12 words), assertive, factual
  - Use it to answer either what was done or what was found
- Abstract
  - Keep it short (~5 to 8 sentences). Write a first version before starting the paper, then a new version after you have finished the paper.
  - It should contain what you did and what you found.
- Introduction
  - Aim for 5-7 paragraphs. Last one starting with 'In this letter/article/...'
  - This is where you sell the idea of the paper. Frequently, is the part that takes longer to write... It answers why we want to perform the work and puts it in context
- Experimental set up
- Analysis
  - As long as necessary, but not longer ...
  - This is your work. It has to be clear and complete.
- Results
  - Keep it short and factual
  - Make sure the results can be used even if our understanding of the issues at hand changes: include tables with as many numbers as possible ...
- Discussion
  - As long as necessary, but not longer ...
  - Compare to expectations and models in a clear and factual way. Enumerate all caveats in the comparison. Based on this, conclude on what we learn and how we could proceed for the next steps.
- Summary/Conclusions/Outlook

Structure of an article

Title

Short (~12 words), assertive, factual

Use it to answer either what was done or what was found

Abstract

Keep it short (~5 to 8 sentences). Write a first version before starting the paper, then a new version after you have finished the paper.

It should contain what you did and what you found.

Introduction

Aim for 5-7 paragraphs. Last one starting with 'In this letter/article/...'

This is where you sell the idea of the paper. Frequently, is the part that takes longer to write... It answers why we want to perform the work and puts it in context

Experimental set up

Analysis

As long as necessary, but not longer ...

This is your work. It has to be clear and complete.

Results

Keep it short and factual

Make sure the results can be used even if our understanding of the issues at hand changes: include tables with as many numbers as possible ...

Discussion

Summary/Conclusions/Outlook

As long as necessary, but not longer ...

Compare to expectations and models in a clear and factual way. Enumerate all caveats in the comparison. Based on this, conclude on what we learn and how we could proceed for the next steps.

Acknowledgments

Appendices

References

Structure of an article

Not necessarily reflected in the actual sections, subsections and so on ...

- Title
- Abstract
- Introduction
- Experimental set up
- Analysis
- Results
- Discussion
- Summary/Conclusions/Outlook
- Acknowledgments
- Appendices
- References

Short (~12 words), assertive, factual

Use it to answer either what was done or what was found

Keep it short (~5 to 8 sentences). Write a first version before starting the paper, then a new version after you have finished the paper.

It should contain what you did and what you found.

Aim for 5-7 paragraphs. Last one starting with 'In this letter/article/...'

This is where you sell the idea of the paper. Frequently, is the part that takes longer to write... It answers why we want to perform the work and puts it in context

As long as necessary, but not longer ...

This is your work. It has to be clear and complete.

Keep it short and factual

Make sure the results can be used even if our understanding of the issues at hand changes: include tables with as many numbers as possible ...

As long as necessary, but not longer ...

Compare to expectations and models in a clear and factual way. Enumerate all caveats in the comparison. Based on this, conclude on what we learn and how we could proceed for the next steps.

Structure of an article

Define spelling and conventions, define the journal, define structure (figs/tabs), then write ...

Not necessarily reflected in the actual sections, subsections and so on ...

- **Title** — Short (~12 words), assertive, factual
  - Use it to answer either what was done or what was found
- **Abstract** — Keep it short (~5 to 8 sentences). Write a first version before starting the paper, then a new version after you have finished the paper.
  - It should contain what you did and what you found.
- **Introduction** — Aim for 5-7 paragraphs. Last one starting with 'In this letter/article/...'
  - This is where you sell the idea of the paper. Frequently, is the part that takes longer to write... It answers why we want to perform the work and puts it in context
- **Experimental set up**
- **Analysis**
  - (Experimental set up and Analysis) As long as necessary, but not longer ...
  - This is your work. It has to be clear and complete.
- **Results** — Keep it short and factual
  - Make sure the results can be used even if our understanding of the issues at hand changes: include tables with as many numbers as possible ...
- **Discussion** — As long as necessary, but not longer ...
  - Compare to expectations and models in a clear and factual way. Enumerate all caveats in the comparison. Based on this, conclude on what we learn and how we could proceed for the next steps.
- **Summary/Conclusions/Outlook**
- **Acknowledgments**
- **Appendices**
- **References**

Journals

Letters

Articles

Instrumentation

Others

Journals

Letters

PRL

Wide audience, large 'impact factor', strict page limits, normally 3 referees, motivation letter needed

PLB

More specialised than PRL. More flexibility in the length. Also high impact.

Articles

Instrumentation

Others

Journals

Letters

PRL

Wide audience, large 'impact factor', strict page limits, normally 3 referees, motivation letter needed

PLB

More specialised than PRL. More flexibility in the length. Also high impact.

Articles

PRC, PRD

Specialised relatives of PRL (APS family). C=nuclear, D=protons

JHEP

EJPA, EJPC

Instrumentation

Others

Journals

Letters

- PRL
- PLB

Wide audience, large 'impact factor', strict page limits, normally 3 referees, motivation letter needed

More specialised than PRL. More flexibility in the length. Also high impact.

Articles

- PRC, PRD
- JHEP
- EJPA, EJPC

Specialised relatives of PRL (APS family). C=nuclear, D=protons

Instrumentation

- JINST
- NIM

Others

Journals

Letters

PRL

Wide audience, large 'impact factor', strict page limits, normally 3 referees, motivation letter needed

PLB

More specialised than PRL. More flexibility in the length. Also high impact.

Articles

PRC, PRD

Specialised relatives of PRL (APS family). C=nuclear, D=protons

JHEP

EJPA, EJPC

Instrumentation

JINST

NIM

Others

Nature

Various members in the family (eg Nature Physics). Wide audience, embargo, not open access (unless you pay several thousand euros). Only 'spectacular' results accepted (there should be impact in other areas) ... USA variant: Science.

Learn to count

How many pages?
How many paragraphs?
How many sentences?
How many figures/tables?

Learn to count

Submitted to JHEP. Some 20 pages in ALICE format.
Five figures, five (large) tables, 85 references ...

How many pages?
How many paragraphs?
How many sentences?
How many figures/tables?

arxiv: 2305.19060

Energy dependence of coherent photonuclear production of J/ψ mesons in ultra-peripheral Pb–Pb collisions at $\sqrt{s_{NN}} = 5.02$ TeV

Learn to count

How many pages?
How many paragraphs?
How many sentences?
How many figures/tables?

Submitted to JHEP. Some 20 pages in ALICE format.
Five figures, five (large) tables, 85 references ...

arxiv: 2305.19060

Energy dependence of coherent photonuclear production of J/ψ mesons in ultra-peripheral Pb–Pb collisions at $\sqrt{s_{NN}} = 5.02$ TeV

Submitted to PRL. Some 7 pages in ALICE format.
Two figures, two (smallish) tables, 47 references ...

arxiv: 2305.06169

First measurement of the $|t|$-dependence of incoherent J/ψ photonuclear production

JHEP example

JHEP

PUBLISHED FOR SISSA BY SPRINGER

RECEIVED: *March 1, 2020*
REVISED: *April 2, 2020*
ACCEPTED: *May 11, 2020*
PUBLISHED: *June 4, 2020*

Coherent photoproduction of ρ^0 vector mesons in ultra-peripheral Pb-Pb collisions at $\sqrt{s_{\rm NN}} = 5.02$ TeV

ALICE

The ALICE collaboration

E-mail: ALICE-publications@cern.ch

ABSTRACT: Cross sections for the coherent photoproduction of ρ^0 vector mesons in ultra-peripheral Pb-Pb collisions at $\sqrt{s_{\rm NN}} = 5.02$ TeV are reported. The measurements, which rely on the $\pi^+\pi^-$ decay channel, are presented in three regions of rapidity covering the range $|y| < 0.8$. For each rapidity interval, cross sections are shown for different nuclear-breakup classes defined according to the presence of neutrons measured in the zero-degree calorimeters. The results are compared with predictions based on different models of nuclear shadowing. Finally, the observation of a coherently produced resonance-like structure with a mass around 1.7 GeV/c^2 and a width of about 140 MeV/c^2 is reported and compared with similar observations from other experiments.

KEYWORDS: Heavy Ion Experiments, Heavy-ion collision, Particle and resonance production

ARXIV EPRINT: 2002.10897

https://doi.org/10.1007/JHEP06(2020)035

Contents

1 Introduction

The electromagnetic field of a fast charged particle, such as those circulating in the Large Hadron Collider (LHC), is strongly Lorentz-contracted and its strength is dominated by the component perpendicular to the direction of motion, such that it can be described as a flux of quasi-real photons. The intensity of this photon flux is proportional to the square of the electric charge of the particle; thus when lead ions circulate in the LHC there are, in addition to the standard hadronic collisions, also copious photonuclear interactions. Ultra-peripheral collisions (UPC) are defined as those for which the impact parameter is larger than the sum of the radii of the incoming particles, in which case the occurrence of hadronic processes is strongly suppressed due to the short range nature of quantum chromodynamics (QCD), and photon-induced processes dominate the interaction rate. The physics of UPC and recent results obtained at the LHC are reviewed in [1, 2].

The photonuclear production of a ρ^0 vector meson in Pb-Pb UPC at the LHC is particularly interesting, because its large cross section makes it a good tool to study the approach to the black-disk limit of QCD [3]. This process can be pictured as follows: a quasi-real photon, emitted by one of the Pb ions, fluctuates into a QCD object which

– 1 –

JHEP06(2020)035

JHEP uses single column format.
No limits on the number of pages/tables/figures
Includes a table of content

JHEP example


JHEP
Published for SISSA by Springer
Received: March 1, 2020
Revised: April 2, 2020
Accepted: May 11, 2020
Published: June 4, 2020

Coherent photoproduction of ρ^0 vector mesons in ultra-peripheral Pb-Pb collisions at $\sqrt{s_{\rm NN}} = 5.02$ TeV

ALICE
The ALICE collaboration

E-mail: ALICE-publications@cern.ch

Abstract: Cross sections for the coherent photoproduction of ρ^0 vector mesons in ultra-peripheral Pb-Pb collisions at $\sqrt{s_{\rm NN}} = 5.02$ TeV are reported. The measurements, which rely on the $\pi^+\pi^-$ decay channel, are presented in three regions of rapidity covering the range $|y| < 0.8$. For each rapidity interval, cross sections are shown for different nuclear-breakup classes defined according to the presence of neutrons measured in the zero-degree calorimeters. The results are compared with predictions based on different models of nuclear shadowing. Finally, the observation of a coherently produced resonance-like structure with a mass around 1.7 GeV/c^2 and a width of about 140 MeV/c^2 is reported and compared with similar observations from other experiments.

Keywords: Heavy Ion Experiments, Heavy-ion collision, Particle and resonance production

ArXiv ePrint: 2002.10897

https://doi.org/10.1007/JHEP06(2020)035

Contents

1 Introduction

The electromagnetic field of a fast charged particle, such as those circulating in the Large Hadron Collider (LHC), is strongly Lorentz-contracted and its strength is dominated by the component perpendicular to the direction of motion, such that it can be described as a flux of quasi-real photons. The intensity of this photon flux is proportional to the square of the electric charge of the particle; thus when lead ions circulate in the LHC there are, in addition to the standard hadronic collisions, also copious photonuclear interactions. Ultra-peripheral collisions (UPC) are defined as those for which the impact parameter is larger than the sum of the radii of the incoming particles, in which case the occurrence of hadronic processes is strongly suppressed due to the short range nature of quantum chromodynamics (QCD), and photon-induced processes dominate the interaction rate. The physics of UPC and recent results obtained at the LHC are reviewed in [1, 2].

The photonuclear production of a ρ^0 vector meson in Pb-Pb UPC at the LHC is particularly interesting, because its large cross section makes it a good tool to study the approach to the black-disk limit of QCD [3]. This process can be pictured as follows: a quasi-real photon, emitted by one of the Pb ions, fluctuates into a QCD object which

JHEP06(2020)035

JHEP uses single column format.
No limits on the number of pages/tables/figures
Includes a table of content

Some 15 words per line
Some 40 lines per page
≈ some 600 words per page ...

how many words do **you** use in a normal sentence?

PRL example

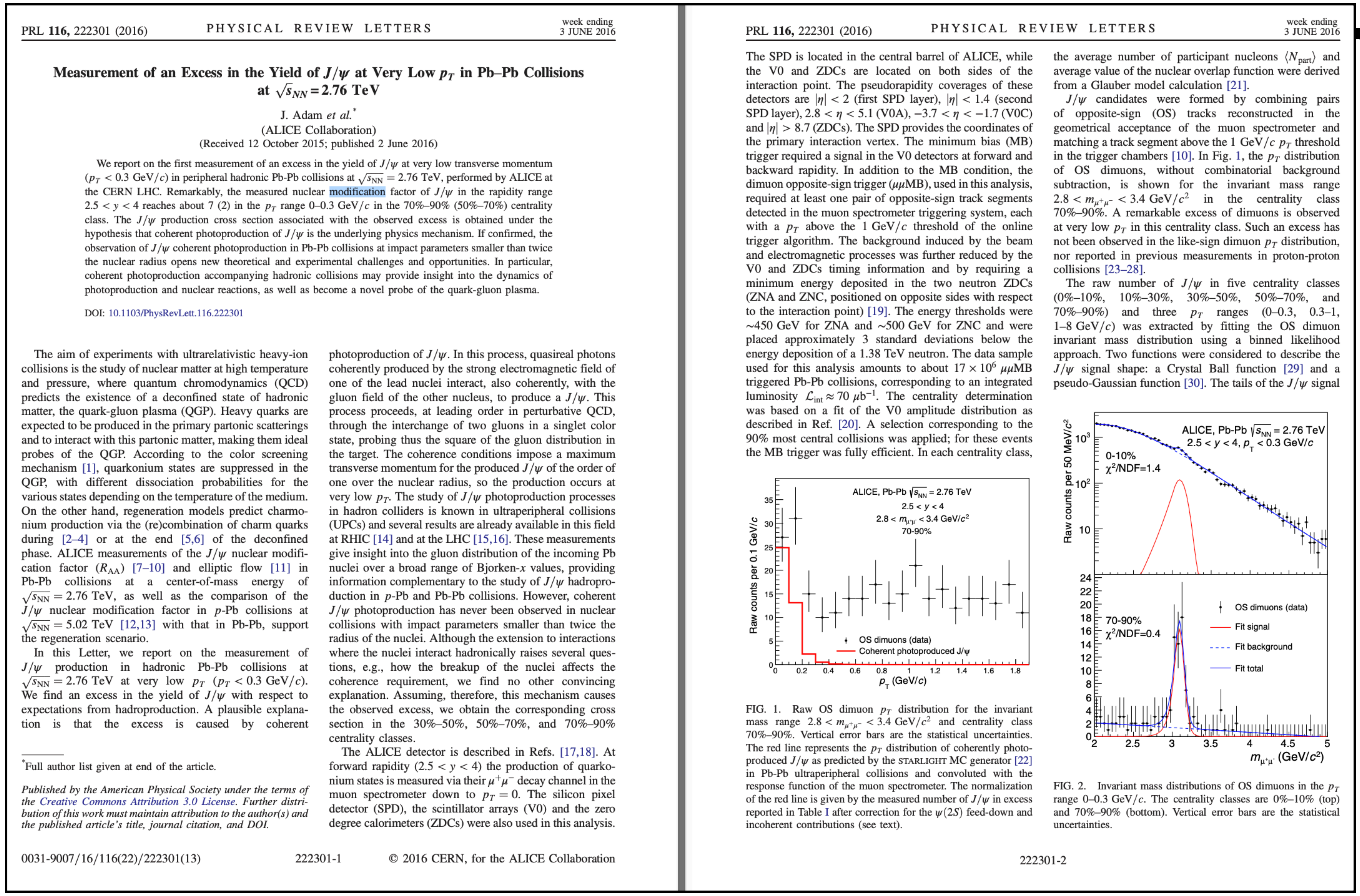

PRL **116,** 222301 (2016) PHYSICAL REVIEW LETTERS week ending 3 JUNE 2016

Measurement of an Excess in the Yield of J/ψ at Very Low p_T in Pb–Pb Collisions at $\sqrt{s_{NN}} = 2.76$ TeV

J. Adam *et al.**

(ALICE Collaboration)

(Received 12 October 2015; published 2 June 2016)

We report on the first measurement of an excess in the yield of J/ψ at very low transverse momentum ($p_T < 0.3$ GeV/c) in peripheral hadronic Pb-Pb collisions at $\sqrt{s_{NN}} = 2.76$ TeV, performed by ALICE at the CERN LHC. Remarkably, the measured nuclear modification factor of J/ψ in the rapidity range $2.5 < y < 4$ reaches about 7 (2) in the p_T range 0–0.3 GeV/c in the 70%–90% (50%–70%) centrality class. The J/ψ production cross section associated with the observed excess is obtained under the hypothesis that coherent photoproduction of J/ψ is the underlying physics mechanism. If confirmed, the observation of J/ψ coherent photoproduction in Pb-Pb collisions at impact parameters smaller than twice the nuclear radius opens new theoretical and experimental challenges and opportunities. In particular, coherent photoproduction accompanying hadronic collisions may provide insight into the dynamics of photoproduction and nuclear reactions, as well as become a novel probe of the quark-gluon plasma.

DOI: 10.1103/PhysRevLett.116.222301

The aim of experiments with ultrarelativistic heavy-ion collisions is the study of nuclear matter at high temperature and pressure, where quantum chromodynamics (QCD) predicts the existence of a deconfined state of hadronic matter, the quark-gluon plasma (QGP). Heavy quarks are expected to be produced in the primary partonic scatterings and to interact with this partonic matter, making them ideal probes of the QGP. According to the color screening mechanism [1], quarkonium states are suppressed in the QGP, with different dissociation probabilities for the various states depending on the temperature of the medium. On the other hand, regeneration models predict charmonium production via the (re)combination of charm quarks during [2–4] or at the end [5,6] of the deconfined phase. ALICE measurements of the J/ψ nuclear modification factor (R_{AA}) [7–10] and elliptic flow [11] in Pb-Pb collisions at a center-of-mass energy of $\sqrt{s_{NN}} = 2.76$ TeV, as well as the comparison of the J/ψ nuclear modification factor in p-Pb collisions at $\sqrt{s_{NN}} = 5.02$ TeV [12,13] with that in Pb-Pb, support the regeneration scenario.

In this Letter, we report on the measurement of J/ψ production in hadronic Pb-Pb collisions at $\sqrt{s_{NN}} = 2.76$ TeV at very low p_T ($p_T < 0.3$ GeV/c). We find an excess in the yield of J/ψ with respect to expectations from hadroproduction. A plausible explanation is that the excess is caused by coherent photoproduction of J/ψ. In this process, quasireal photons coherently produced by the strong electromagnetic field of one of the lead nuclei interact, also coherently, with the gluon field of the other nucleus, to produce a J/ψ. This process proceeds, at leading order in perturbative QCD, through the interchange of two gluons in a singlet color state, probing thus the square of the gluon distribution in the target. The coherence conditions impose a maximum transverse momentum for the produced J/ψ of the order of one over the nuclear radius, so the production occurs at very low p_T. The study of J/ψ photoproduction processes in hadron colliders is known in ultraperipheral collisions (UPCs) and several results are already available in this field at RHIC [14] and at the LHC [15,16]. These measurements give insight into the gluon distribution of the incoming Pb nuclei over a broad range of Bjorken-x values, providing information complementary to the study of J/ψ hadroproduction in p-Pb and Pb-Pb collisions. However, coherent J/ψ photoproduction has never been observed in nuclear collisions with impact parameters smaller than twice the radius of the nuclei. Although the extension to interactions where the nuclei interact hadronically raises several questions, e.g., how the breakup of the nuclei affects the coherence requirement, we find no other convincing explanation. Assuming, therefore, this mechanism causes the observed excess, we obtain the corresponding cross section in the 30%–50%, 50%–70%, and 70%–90% centrality classes.

The ALICE detector is described in Refs. [17,18]. At forward rapidity ($2.5 < y < 4$) the production of quarkonium states is measured via their $\mu^+\mu^-$ decay channel in the muon spectrometer down to $p_T = 0$. The silicon pixel detector (SPD), the scintillator arrays (V0) and the zero degree calorimeters (ZDCs) were also used in this analysis.

*Full author list given at end of the article.

Published by the American Physical Society under the terms of the Creative Commons Attribution 3.0 License. Further distribution of this work must maintain attribution to the author(s) and the published article's title, journal citation, and DOI.

0031-9007/16/116(22)/222301(13) 222301-1 © 2016 CERN, for the ALICE Collaboration

PRL **116,** 222301 (2016) PHYSICAL REVIEW LETTERS week ending 3 JUNE 2016

The SPD is located in the central barrel of ALICE, while the V0 and ZDCs are located on both sides of the interaction point. The pseudorapidity coverages of these detectors are $|\eta| < 2$ (first SPD layer), $|\eta| < 1.4$ (second SPD layer), $2.8 < \eta < 5.1$ (V0A), $-3.7 < \eta < -1.7$ (V0C) and $|\eta| > 8.7$ (ZDCs). The SPD provides the coordinates of the primary interaction vertex. The minimum bias (MB) trigger required a signal in the V0 detectors at forward and backward rapidity. In addition to the MB condition, the dimuon opposite-sign trigger ($\mu\mu$MB), used in this analysis, required at least one pair of opposite-sign track segments detected in the muon spectrometer triggering system, each with a p_T above the 1 GeV/c threshold of the online trigger algorithm. The background induced by the beam and electromagnetic processes was further reduced by the V0 and ZDCs timing information and by requiring a minimum energy deposited in the two neutron ZDCs (ZNA and ZNC, positioned on opposite sides with respect to the interaction point) [19]. The energy thresholds were ~450 GeV for ZNA and ~500 GeV for ZNC and were placed approximately 3 standard deviations below the energy deposition of a 1.38 TeV neutron. The data sample used for this analysis amounts to about 17×10^6 $\mu\mu$MB triggered Pb-Pb collisions, corresponding to an integrated luminosity $\mathcal{L}_{int} \approx 70\ \mu b^{-1}$. The centrality determination was based on a fit of the V0 amplitude distribution as described in Ref. [20]. A selection corresponding to the 90% most central collisions was applied; for these events the MB trigger was fully efficient. In each centrality class, the average number of participant nucleons $\langle N_{part}\rangle$ and average value of the nuclear overlap function were derived from a Glauber model calculation [21].

J/ψ candidates were formed by combining pairs of opposite-sign (OS) tracks reconstructed in the geometrical acceptance of the muon spectrometer and matching a track segment above the 1 GeV/c p_T threshold in the trigger chambers [10]. In Fig. 1, the p_T distribution of OS dimuons, without combinatorial background subtraction, is shown for the invariant mass range $2.8 < m_{\mu^+\mu^-} < 3.4$ GeV/c^2 in the centrality class 70%–90%. A remarkable excess of dimuons is observed at very low p_T in this centrality class. Such an excess has not been observed in the like-sign dimuon p_T distribution, nor reported in previous measurements in proton-proton collisions [23–28].

The raw number of J/ψ in five centrality classes (0%–10%, 10%–30%, 30%–50%, 50%–70%, and 70%–90%) and three p_T ranges (0–0.3, 0.3–1, 1–8 GeV/c) was extracted by fitting the OS dimuon invariant mass distribution using a binned likelihood approach. Two functions were considered to describe the J/ψ signal shape: a Crystal Ball function [29] and a pseudo-Gaussian function [30]. The tails of the J/ψ signal

FIG. 1. Raw OS dimuon p_T distribution for the invariant mass range $2.8 < m_{\mu^+\mu^-} < 3.4$ GeV/c^2 and centrality class 70%–90%. Vertical error bars are the statistical uncertainties. The red line represents the p_T distribution of coherently photoproduced J/ψ as predicted by the STARLIGHT MC generator [22] in Pb-Pb ultraperipheral collisions and convoluted with the response function of the muon spectrometer. The normalization of the red line is given by the measured number of J/ψ in excess reported in Table I after correction for the $\psi(2S)$ feed-down and incoherent contributions (see text).

FIG. 2. Invariant mass distributions of OS dimuons in the p_T range 0–0.3 GeV/c. The centrality classes are 0%–10% (top) and 70%–90% (bottom). Vertical error bars are the statistical uncertainties.

222301-2

PRL uses double column format.

Strict limit on the number of pages, tables/figures

No ToC, frequently no explicit sectioning

PRL example

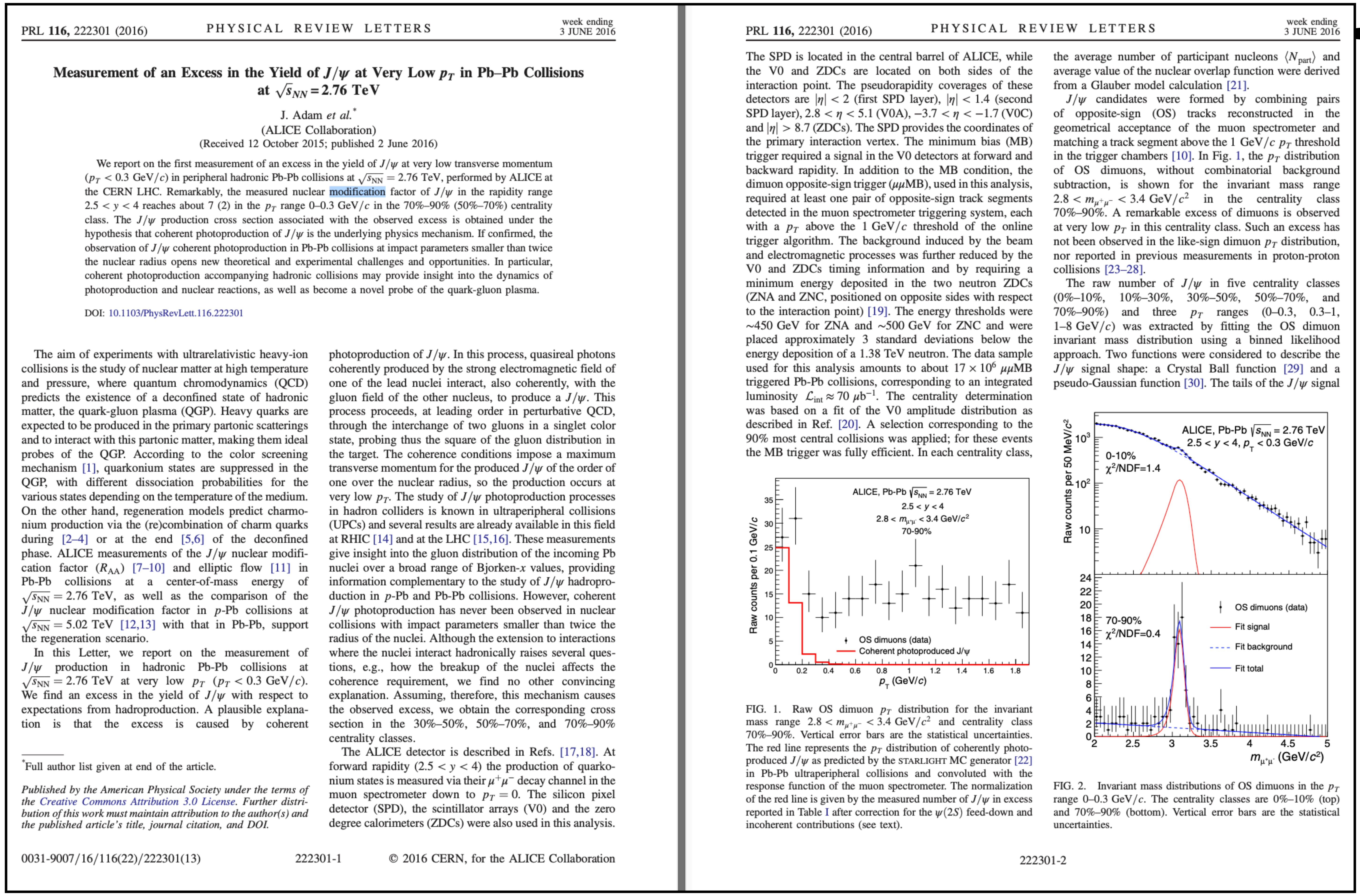
PRL **116,** 222301 (2016) PHYSICAL REVIEW LETTERS week ending 3 JUNE 2016

Measurement of an Excess in the Yield of J/ψ at Very Low p_T in Pb–Pb Collisions at $\sqrt{s_{NN}} = 2.76$ TeV

J. Adam *et al.*[*]

(ALICE Collaboration)

(Received 12 October 2015; published 2 June 2016)

We report on the first measurement of an excess in the yield of J/ψ at very low transverse momentum ($p_T < 0.3$ GeV/c) in peripheral hadronic Pb-Pb collisions at $\sqrt{s_{NN}} = 2.76$ TeV, performed by ALICE at the CERN LHC. Remarkably, the measured nuclear modification factor of J/ψ in the rapidity range $2.5 < y < 4$ reaches about 7 (2) in the p_T range 0–0.3 GeV/c in the 70%–90% (50%–70%) centrality class. The J/ψ production cross section associated with the observed excess is obtained under the hypothesis that coherent photoproduction of J/ψ is the underlying physics mechanism. If confirmed, the observation of J/ψ coherent photoproduction in Pb-Pb collisions at impact parameters smaller than twice the nuclear radius opens new theoretical and experimental challenges and opportunities. In particular, coherent photoproduction accompanying hadronic collisions may provide insight into the dynamics of photoproduction and nuclear reactions, as well as become a novel probe of the quark-gluon plasma.

DOI: 10.1103/PhysRevLett.116.222301

The aim of experiments with ultrarelativistic heavy-ion collisions is the study of nuclear matter at high temperature and pressure, where quantum chromodynamics (QCD) predicts the existence of a deconfined state of hadronic matter, the quark-gluon plasma (QGP). Heavy quarks are expected to be produced in the primary partonic scatterings and to interact with this partonic matter, making them ideal probes of the QGP. According to the color screening mechanism [1], quarkonium states are suppressed in the QGP, with different dissociation probabilities for the various states depending on the temperature of the medium. On the other hand, regeneration models predict charmonium production via the (re)combination of charm quarks during [2–4] or at the end [5,6] of the deconfined phase. ALICE measurements of the J/ψ nuclear modification factor (R_{AA}) [7–10] and elliptic flow [11] in Pb-Pb collisions at a center-of-mass energy of $\sqrt{s_{NN}} = 2.76$ TeV, as well as the comparison of the J/ψ nuclear modification factor in p-Pb collisions at $\sqrt{s_{NN}} = 5.02$ TeV [12,13] with that in Pb-Pb, support the regeneration scenario.

In this Letter, we report on the measurement of J/ψ production in hadronic Pb-Pb collisions at $\sqrt{s_{NN}} = 2.76$ TeV at very low p_T ($p_T < 0.3$ GeV/c). We find an excess in the yield of J/ψ with respect to expectations from hadroproduction. A plausible explanation is that the excess is caused by coherent photoproduction of J/ψ. In this process, quasireal photons coherently produced by the strong electromagnetic field of one of the lead nuclei interact, also coherently, with the gluon field of the other nucleus, to produce a J/ψ. This process proceeds, at leading order in perturbative QCD, through the interchange of two gluons in a singlet color state, probing thus the square of the gluon distribution in the target. The coherence conditions impose a maximum transverse momentum for the produced J/ψ of the order of one over the nuclear radius, so the production occurs at very low p_T. The study of J/ψ photoproduction processes in hadron colliders is known in ultraperipheral collisions (UPCs) and several results are already available in this field at RHIC [14] and at the LHC [15,16]. These measurements give insight into the gluon distribution of the incoming Pb nuclei over a broad range of Bjorken-x values, providing information complementary to the study of J/ψ hadroproduction in p-Pb and Pb-Pb collisions. However, coherent J/ψ photoproduction has never been observed in nuclear collisions with impact parameters smaller than twice the radius of the nuclei. Although the extension to interactions where the nuclei interact hadronically raises several questions, e.g., how the breakup of the nuclei affects the coherence requirement, we find no other convincing explanation. Assuming, therefore, this mechanism causes the observed excess, we obtain the corresponding cross section in the 30%–50%, 50%–70%, and 70%–90% centrality classes.

The ALICE detector is described in Refs. [17,18]. At forward rapidity ($2.5 < y < 4$) the production of quarkonium states is measured via their $\mu^+\mu^-$ decay channel in the muon spectrometer down to $p_T = 0$. The silicon pixel detector (SPD), the scintillator arrays (V0) and the zero degree calorimeters (ZDCs) were also used in this analysis.

[*]Full author list given at end of the article.

Published by the American Physical Society under the terms of the Creative Commons Attribution 3.0 License. Further distribution of this work must maintain attribution to the author(s) and the published article's title, journal citation, and DOI.

0031-9007/16/116(22)/222301(13) 222301-1 © 2016 CERN, for the ALICE Collaboration

PRL **116,** 222301 (2016) PHYSICAL REVIEW LETTERS week ending 3 JUNE 2016

The SPD is located in the central barrel of ALICE, while the V0 and ZDCs are located on both sides of the interaction point. The pseudorapidity coverages of these detectors are $|\eta| < 2$ (first SPD layer), $|\eta| < 1.4$ (second SPD layer), $2.8 < \eta < 5.1$ (V0A), $-3.7 < \eta < -1.7$ (V0C) and $|\eta| > 8.7$ (ZDCs). The SPD provides the coordinates of the primary interaction vertex. The minimum bias (MB) trigger required a signal in the V0 detectors at forward and backward rapidity. In addition to the MB condition, the dimuon opposite-sign trigger ($\mu\mu$MB), used in this analysis, required at least one pair of opposite-sign track segments detected in the muon spectrometer triggering system, each with a p_T above the 1 GeV/c threshold of the online trigger algorithm. The background induced by the beam and electromagnetic processes was further reduced by the V0 and ZDCs timing information and by requiring a minimum energy deposited in the two neutron ZDCs (ZNA and ZNC, positioned on opposite sides with respect to the interaction point) [19]. The energy thresholds were ~450 GeV for ZNA and ~500 GeV for ZNC and were placed approximately 3 standard deviations below the energy deposition of a 1.38 TeV neutron. The data sample used for this analysis amounts to about 17×10^6 $\mu\mu$MB triggered Pb-Pb collisions, corresponding to an integrated luminosity $\mathcal{L}_{int} \approx 70\ \mu b^{-1}$. The centrality determination was based on a fit of the V0 amplitude distribution as described in Ref. [20]. A selection corresponding to the 90% most central collisions was applied; for these events the MB trigger was fully efficient. In each centrality class, the average number of participant nucleons $\langle N_{part}\rangle$ and average value of the nuclear overlap function were derived from a Glauber model calculation [21].

J/ψ candidates were formed by combining pairs of opposite-sign (OS) tracks reconstructed in the geometrical acceptance of the muon spectrometer and matching a track segment above the 1 GeV/c p_T threshold in the trigger chambers [10]. In Fig. 1, the p_T distribution of OS dimuons, without combinatorial background subtraction, is shown for the invariant mass range $2.8 < m_{\mu^+\mu^-} < 3.4$ GeV/c^2 in the centrality class 70%–90%. A remarkable excess of dimuons is observed at very low p_T in this centrality class. Such an excess has not been observed in the like-sign dimuon p_T distribution, nor reported in previous measurements in proton-proton collisions [23–28].

The raw number of J/ψ in five centrality classes (0%–10%, 10%–30%, 30%–50%, 50%–70%, and 70%–90%) and three p_T ranges (0–0.3, 0.3–1, 1–8 GeV/c) was extracted by fitting the OS dimuon invariant mass distribution using a binned likelihood approach. Two functions were considered to describe the J/ψ signal shape: a Crystal Ball function [29] and a pseudo-Gaussian function [30]. The tails of the J/ψ signal

FIG. 1. Raw OS dimuon p_T distribution for the invariant mass range $2.8 < m_{\mu^+\mu^-} < 3.4$ GeV/c^2 and centrality class 70%–90%. Vertical error bars are the statistical uncertainties. The red line represents the p_T distribution of coherently photoproduced J/ψ as predicted by the STARLIGHT MC generator [22] in Pb-Pb ultraperipheral collisions and convoluted with the response function of the muon spectrometer. The normalization of the red line is given by the measured number of J/ψ in excess reported in Table I after correction for the $\psi(2S)$ feed-down and incoherent contributions (see text).

FIG. 2. Invariant mass distributions of OS dimuons in the p_T range 0–0.3 GeV/c. The centrality classes are 0%–10% (top) and 70%–90% (bottom). Vertical error bars are the statistical uncertainties.

222301-2

PRL uses double column format.
Strict limit on the number of pages, tables/figures
No ToC, frequently no explicit sectioning

Some 9 words per line (in one column)
Some 55 lines per page
≈ some 1000 words per page ...

Figures/tables take a lot of text space!

Titles from a recent Nature Physics ToC

Latest Research articles >

Article
31 Jul 2023

Josephson diode effect derived from short-range coherent coupling

The behaviour of a superconductor can be altered by changing its symmetry properties. Coherently coupling two Josephson junctions breaks time-reversal and inversion symmetries, giving rise to a device with a controllable superconducting diode effect.

Sadashige Matsuo, Takaya Imoto ... Seigo Tarucha

Article
31 Jul 2023

Measuring the scattering tensor of a disordered nonlinear medium

Disordered media with their numerous scattering channels can be used as optical operators. Measurements of the scattering tensor of a second-harmonic medium extend this computing application to the nonlinear regime.

Jungho Moon, Ye-Chan Cho ... Wonshik Choi

Article
31 Jul 2023

Magnetic trapping of ultracold molecules at high density

Many applications of ultracold molecules require high densities that have been difficult to reach. An experiment now demonstrates the tight magnetic confinement of ultracold molecules, enabling the study of molecular collisions in the quantum regime.

Juliana J. Park, Yu-Kun Lu ... Wolfgang Ketterle

Article
Open Access
31 Jul 2023

Critical slowing down near a magnetic quantum phase transition with fermionic breakdown

$YbRh_2Si_2$ has a quantum phase transition between an antiferromagnetic phase and a so-called heavy-Fermi-liquid state. Measurements of critical slowing down suggest that the heavy-fermion quasiparticles break down at the transition.

Chia-Jung Yang, Kristin Kliemt ... Shovon Pal

Article
27 Jul 2023

A thermodynamic explanation of the Invar effect

The iron–nickel alloy Invar has an extremely small coefficient of thermal expansion that has been difficult to explain theoretically. A study of Invar under pressure now suggests that there is a cancellation of phonon and spin contributions to expansion.

S. H. Lohaus, M. Heine ... B. Fultz

Titles from a recent Nature Physics ToC

Latest Research articles >

9 words

Article
31 Jul 2023

Josephson diode effect derived from short-range coherent coupling

The behaviour of a superconductor can be altered by changing its symmetry properties. Coherently coupling two Josephson junctions breaks time-reversal and inversion symmetries, giving rise to a device with a controllable superconducting diode effect.

Sadashige Matsuo, Takaya Imoto ... Seigo Tarucha

Article
31 Jul 2023

Measuring the scattering tensor of a disordered nonlinear medium

Disordered media with their numerous scattering channels can be used as optical operators. Measurements of the scattering tensor of a second-harmonic medium extend this computing application to the nonlinear regime.

Jungho Moon, Ye-Chan Cho ... Wonshik Choi

Article
31 Jul 2023

Magnetic trapping of ultracold molecules at high density

Many applications of ultracold molecules require high densities that have been difficult to reach. An experiment now demonstrates the tight magnetic confinement of ultracold molecules, enabling the study of molecular collisions in the quantum regime.

Juliana J. Park, Yu-Kun Lu ... Wolfgang Ketterle

Article
Open Access
31 Jul 2023

Critical slowing down near a magnetic quantum phase transition with fermionic breakdown

$YbRh_2Si_2$ has a quantum phase transition between an antiferromagnetic phase and a so-called heavy-Fermi-liquid state. Measurements of critical slowing down suggest that the heavy-fermion quasiparticles break down at the transition.

Chia-Jung Yang, Kristin Kliemt ... Shovon Pal

Article
27 Jul 2023

A thermodynamic explanation of the Invar effect

The iron–nickel alloy Invar has an extremely small coefficient of thermal expansion that has been difficult to explain theoretically. A study of Invar under pressure now suggests that there is a cancellation of phonon and spin contributions to expansion.

S. H. Lohaus, M. Heine ... B. Fultz

Titles from a recent Nature Physics ToC

Latest Research articles >

Article
31 Jul 2023

Josephson diode effect derived from short-range coherent coupling

The behaviour of a superconductor can be altered by changing its symmetry properties. Coherently coupling two Josephson junctions breaks time-reversal and inversion symmetries, giving rise to a device with a controllable superconducting diode effect.

Sadashige Matsuo, Takaya Imoto ... Seigo Tarucha

9 words

Article
31 Jul 2023

Measuring the scattering tensor of a disordered nonlinear medium

Disordered media with their numerous scattering channels can be used as optical operators. Measurements of the scattering tensor of a second-harmonic medium extend this computing application to the nonlinear regime.

Jungho Moon, Ye-Chan Cho ... Wonshik Choi

9 words

Article
31 Jul 2023

Magnetic trapping of ultracold molecules at high density

Many applications of ultracold molecules require high densities that have been difficult to reach. An experiment now demonstrates the tight magnetic confinement of ultracold molecules, enabling the study of molecular collisions in the quantum regime.

Juliana J. Park, Yu-Kun Lu ... Wolfgang Ketterle

Article
Open Access
31 Jul 2023

Critical slowing down near a magnetic quantum phase transition with fermionic breakdown

$YbRh_2Si_2$ has a quantum phase transition between an antiferromagnetic phase and a so-called heavy-Fermi-liquid state. Measurements of critical slowing down suggest that the heavy-fermion quasiparticles break down at the transition.

Chia-Jung Yang, Kristin Kliemt ... Shovon Pal

Article
27 Jul 2023

A thermodynamic explanation of the Invar effect

The iron–nickel alloy Invar has an extremely small coefficient of thermal expansion that has been difficult to explain theoretically. A study of Invar under pressure now suggests that there is a cancellation of phonon and spin contributions to expansion.

S. H. Lohaus, M. Heine ... B. Fultz

Titles from a recent Nature Physics ToC

Latest Research articles >

Article
31 Jul 2023

Josephson diode effect derived from short-range coherent coupling

9 words

The behaviour of a superconductor can be altered by changing its symmetry properties. Coherently coupling two Josephson junctions breaks time-reversal and inversion symmetries, giving rise to a device with a controllable superconducting diode effect.

Sadashige Matsuo, Takaya Imoto ... Seigo Tarucha

Article
31 Jul 2023

Measuring the scattering tensor of a disordered nonlinear medium

9 words

Disordered media with their numerous scattering channels can be used as optical operators. Measurements of the scattering tensor of a second-harmonic medium extend this computing application to the nonlinear regime.

Jungho Moon, Ye-Chan Cho ... Wonshik Choi

Article
31 Jul 2023

Magnetic trapping of ultracold molecules at high density

8 words

Many applications of ultracold molecules require high densities that have been difficult to reach. An experiment now demonstrates the tight magnetic confinement of ultracold molecules, enabling the study of molecular collisions in the quantum regime.

Juliana J. Park, Yu-Kun Lu ... Wolfgang Ketterle

Article
Open Access
31 Jul 2023

Critical slowing down near a magnetic quantum phase transition with fermionic breakdown

$YbRh_2Si_2$ has a quantum phase transition between an antiferromagnetic phase and a so-called heavy-Fermi-liquid state. Measurements of critical slowing down suggest that the heavy-fermion quasiparticles break down at the transition.

Chia-Jung Yang, Kristin Kliemt ... Shovon Pal

Article
27 Jul 2023

A thermodynamic explanation of the Invar effect

The iron–nickel alloy Invar has an extremely small coefficient of thermal expansion that has been difficult to explain theoretically. A study of Invar under pressure now suggests that there is a cancellation of phonon and spin contributions to expansion.

S. H. Lohaus, M. Heine ... B. Fultz

Titles from a recent Nature Physics ToC

Latest Research articles >

Article
31 Jul 2023

Josephson diode effect derived from short-range coherent coupling

9 words

The behaviour of a superconductor can be altered by changing its symmetry properties. Coherently coupling two Josephson junctions breaks time-reversal and inversion symmetries, giving rise to a device with a controllable superconducting diode effect.

Sadashige Matsuo, Takaya Imoto ... Seigo Tarucha

Article
31 Jul 2023

Measuring the scattering tensor of a disordered nonlinear medium

9 words

Disordered media with their numerous scattering channels can be used as optical operators. Measurements of the scattering tensor of a second-harmonic medium extend this computing application to the nonlinear regime.

Jungho Moon, Ye-Chan Cho ... Wonshik Choi

Article
31 Jul 2023

Magnetic trapping of ultracold molecules at high density

8 words

Many applications of ultracold molecules require high densities that have been difficult to reach. An experiment now demonstrates the tight magnetic confinement of ultracold molecules, enabling the study of molecular collisions in the quantum regime.

Juliana J. Park, Yu-Kun Lu ... Wolfgang Ketterle

Article
Open Access
31 Jul 2023

Critical slowing down near a magnetic quantum phase transition with fermionic breakdown

12 words

$YbRh_2Si_2$ has a quantum phase transition between an antiferromagnetic phase and a so-called heavy-Fermi-liquid state. Measurements of critical slowing down suggest that the heavy-fermion quasiparticles break down at the transition.

Chia-Jung Yang, Kristin Kliemt ... Shovon Pal

Article
27 Jul 2023

A thermodynamic explanation of the Invar effect

The iron–nickel alloy Invar has an extremely small coefficient of thermal expansion that has been difficult to explain theoretically. A study of Invar under pressure now suggests that there is a cancellation of phonon and spin contributions to expansion.

S. H. Lohaus, M. Heine ... B. Fultz

Titles from a recent Nature Physics ToC

Latest Research articles >

Article
31 Jul 2023

Josephson diode effect derived from short-range coherent coupling

The behaviour of a superconductor can be altered by changing its symmetry properties. Coherently coupling two Josephson junctions breaks time-reversal and inversion symmetries, giving rise to a device with a controllable superconducting diode effect.

Sadashige Matsuo, Takaya Imoto ... Seigo Tarucha

9 words

Article
31 Jul 2023

Measuring the scattering tensor of a disordered nonlinear medium

Disordered media with their numerous scattering channels can be used as optical operators. Measurements of the scattering tensor of a second-harmonic medium extend this computing application to the nonlinear regime.

Jungho Moon, Ye-Chan Cho ... Wonshik Choi

9 words

Article
31 Jul 2023

Magnetic trapping of ultracold molecules at high density

Many applications of ultracold molecules require high densities that have been difficult to reach. An experiment now demonstrates the tight magnetic confinement of ultracold molecules, enabling the study of molecular collisions in the quantum regime.

Juliana J. Park, Yu-Kun Lu ... Wolfgang Ketterle

8 words

Article
Open Access
31 Jul 2023

Critical slowing down near a magnetic quantum phase transition with fermionic breakdown

$YbRh_2Si_2$ has a quantum phase transition between an antiferromagnetic phase and a so-called heavy-Fermi-liquid state. Measurements of critical slowing down suggest that the heavy-fermion quasiparticles break down at the transition.

Chia-Jung Yang, Kristin Kliemt ... Shovon Pal

12 words

Article
27 Jul 2023

A thermodynamic explanation of the Invar effect

The iron–nickel alloy Invar has an extremely small coefficient of thermal expansion that has been difficult to explain theoretically. A study of Invar under pressure now suggests that there is a cancellation of phonon and spin contributions to expansion.

S. H. Lohaus, M. Heine ... B. Fultz

7 words

Titles from a recent Nature Physics ToC

Latest Research articles >

Article
31 Jul 2023

Josephson diode effect derived from short-range coherent coupling

The behaviour of a superconductor can be altered by changing its symmetry properties. Coherently coupling two Josephson junctions breaks time-reversal and inversion symmetries, giving rise to a device with a controllable superconducting diode effect.

Sadashige Matsuo, Takaya Imoto ... Seigo Tarucha

9 words

Article
31 Jul 2023

Measuring the scattering tensor of a disordered nonlinear medium

Disordered media with their numerous scattering channels can be used as optical operators. Measurements of the scattering tensor of a second-harmonic medium extend this computing application to the nonlinear regime.

Jungho Moon, Ye-Chan Cho ... Wonshik Choi

9 words

Article
31 Jul 2023

Magnetic trapping of ultracold molecules at high density

Many applications of ultracold molecules require high densities that have been difficult to reach. An experiment now demonstrates the tight magnetic confinement of ultracold molecules, enabling the study of molecular collisions in the quantum regime.

Juliana J. Park, Yu-Kun Lu ... Wolfgang Ketterle

8 words

Article
Open Access
31 Jul 2023

Critical slowing down near a magnetic quantum phase transition with fermionic breakdown

$YbRh_2Si_2$ has a quantum phase transition between an antiferromagnetic phase and a so-called heavy-Fermi-liquid state. Measurements of critical slowing down suggest that the heavy-fermion quasiparticles break down at the transition.

Chia-Jung Yang, Kristin Kliemt ... Shovon Pal

12 words

Article
27 Jul 2023

A thermodynamic explanation of the Invar effect

The iron–nickel alloy Invar has an extremely small coefficient of thermal expansion that has been difficult to explain theoretically. A study of Invar under pressure now suggests that there is a cancellation of phonon and spin contributions to expansion.

S. H. Lohaus, M. Heine ... B. Fultz

7 words

Which one of these titles do you like best and why

Let's look at one paper

Physics Letters B 817 (2021) 136280

Contents lists available at ScienceDirect

Physics Letters B

www.elsevier.com/locate/physletb

ELSEVIER

First measurement of the $|t|$-dependence of coherent J/ψ photonuclear production

Check for updates

ALICE Collaboration *

ARTICLE INFO

Article history:
Received 24 January 2021
Received in revised form 17 March 2021
Accepted 6 April 2021
Available online 15 April 2021
Editor: M. Doser

ABSTRACT

The first measurement of the cross section for coherent J/ψ photoproduction as a function of $|t|$, the square of the momentum transferred between the incoming and outgoing target nucleus, is presented. The data were measured with the ALICE detector in ultra-peripheral Pb–Pb collisions at a centre-of-mass energy per nucleon pair $\sqrt{s_{NN}} = 5.02$ TeV with the J/ψ produced in the central rapidity region $|y| < 0.8$, which corresponds to the small Bjorken-x range $(0.3 - 1.4) \times 10^{-3}$.
The measured $|t|$-dependence is not described by computations based only on the Pb nuclear form factor, while the photonuclear cross section is better reproduced by models including shadowing according to the leading-twist approximation, or gluon-saturation effects from the impact-parameter dependent Balitsky–Kovchegov equation. These new results are therefore a valid tool to constrain the relevant model parameters and to investigate the transverse gluonic structure at very low Bjorken-x.

1. Introduction

Photonuclear reactions can be studied in ultra-peripheral collisions (UPCs) of heavy ions where the two projectiles pass each other with an impact parameter larger than the sum of their radii. In this case, purely hadronic interactions are suppressed and electromagnetically induced processes occur via photons with typically very small virtualities, of the order of tens of MeV^2. The intensity of the photon flux is proportional to the square of the electric charge of the nuclei, resulting in large cross sections for the coherent photoproduction of a vector meson in UPCs of Pb ions at the LHC. This process has a clear experimental signature: the decay products of the vector meson are the only particles detected in an otherwise empty detector.

The physics of vector meson photoproduction is described, e.g., in Refs. [1–4]. Two vector meson photoproduction processes, coherent and incoherent, are relevant for the results presented here. In the former, the photon interacts with all nucleons in a nucleus, while in the latter it interacts with a single nucleon. In both cases a single vector meson is produced. Experimentally, one can distinguish between these two production types through the transverse momentum p_T of the vector meson which is related to the transverse size of the target. While coherent photoproduction is characterised by an average transverse momentum $\langle p_T \rangle \sim 60$ MeV/c, incoherent production leads to higher average transverse momenta: $\langle p_T \rangle \sim 500$ MeV/c. Incoherent photoproduction can also be accompanied by the excitation and dissociation of the target nucleon resulting in an even higher transverse momentum of the produced vector meson [5].

Shadowing, the observation that the structure of a nucleon inside nuclear matter is different from that of a free nucleon [6], is not yet completely understood and several processes may have a role in different kinematic regions. In this context, coherent heavy vector meson photoproduction is of particular interest, because it is especially sensitive to the gluon distribution in the target, and thus to gluon shadowing effects at low Bjorken-x [7,8]. One of the effects expected to contribute to shadowing in this kinematic region is saturation, a dynamic equilibrium between gluon radiation and recombination [9]. The momentum scale of the interaction (Q^2) is related to the mass m_V of the vector meson as $Q^2 \sim m_V^2/4$, corresponding to the perturbative regime of quantum chromodynamics (QCD) in the case of charmonium states. The rapidity of the coherently produced $c\bar{c}$ states is related to the Bjorken-x of the gluonic exchange as $x = (m_V/\sqrt{s_{NN}}) \exp(\pm y)$, where the two signs indicate that either of the incoming ions can be the source of the photon. Thus, the charmonium photoproduction cross section at midrapidity in Pb–Pb UPCs at the LHC Run 2 centre-of-mass energy per nucleon pair of $\sqrt{s_{NN}} = 5.02$ TeV is sensitive to $x \in (0.3, 1.4) \times 10^{-3}$ at ALICE. It thereby provides information on the gluon distribution in nuclei in a kinematic region where shadowing could be present and saturation effects may be important [10,11].

Charmonium photoproduction in ultra-peripheral Pb–Pb collisions was previously studied by the ALICE Collaboration at $\sqrt{s_{NN}} = 2.76$ TeV [12–14]. The coherent J/ψ photoproduction cross section was measured both at midrapidity $|y| < 0.9$ and at forward

* E-mail address: alice-publications@cern.ch.

https://doi.org/10.1016/j.physletb.2021.136280

rapidity $-3.6 < y < -2.6$. Recently, a measurement of the rapidity dependence of coherent J/ψ photoproduction at forward rapidity at the higher energy of $\sqrt{s_{NN}} = 5.02$ TeV was also published by the ALICE Collaboration [15]. In addition, the CMS Collaboration studied the coherent J/ψ photoproduction accompanied by neutron emission at semi-forward rapidity $1.8 < |y| < 2.3$ at $\sqrt{s_{NN}} = 2.76$ TeV [16]. These measurements allow for a deeper insight into the rapidity dependence of gluon shadowing, but do not give information on the behaviour of gluons in the impact-parameter plane. The square of the momentum transferred to the target nucleus, $|t|$, is related through a two-dimensional Fourier transform to the gluon distribution in the plane transverse to the interaction [17]; thus the study of the $|t|$-dependence of coherent J/ψ photoproduction provides information about the spatial distribution of gluons as a function of the impact parameter. Thus far, the only measurements in this direction were performed recently by the STAR Collaboration for the case of the ρ^0 vector meson [18] and for the yield of J/ψ in semi-central Au–Au collisions [19].

In this Letter, the first measurement of the $|t|$-dependence of the coherent J/ψ photoproduction cross section at midrapidity in Pb–Pb UPCs at $\sqrt{s_{NN}} = 5.02$ TeV is presented. The J/ψ vector mesons were reconstructed in the rapidity range $|y| < 0.8$ through their decay into $\mu^+\mu^-$, taking advantage of the better mass and momentum resolution of this channel with respect to the e^+e^- channel. The data sample, recorded in 2018, is approximately 10 times larger than that used in previous ALICE measurements at midrapidity at the lower energy of $\sqrt{s_{NN}} = 2.76$ TeV [14]. Cross sections are reported for six $|t|$ intervals and compared with theoretical predictions.

2. Detector description

The ALICE detector and its performance are described in Refs. [20,21]. Three central barrel detectors, the Inner Tracking System (ITS), the Time Projection Chamber (TPC), and the Time-of-Flight (TOF), in addition to two forward detectors, V0 and the ALICE Diffractive (AD) arrays, are used in this analysis. The central barrel detectors are surrounded by a large solenoid magnet producing a magnetic field of $B = 0.5$ T. The V0, AD, ITS, and TOF detectors are used for triggering, the ITS and the TPC for particle tracking, and the TPC for particle identification.

The V0 is a scintillator detector made of two counters, V0A and V0C, installed on both sides of the interaction point. The V0A and V0C cover the pseudorapidity ranges $2.8 < \eta < 5.1$ and $-3.7 < \eta < -1.7$, respectively. Both counters are segmented in four rings in the radial direction, with each ring divided into 8 sections in azimuth.

The AD consists of two scintillator stations, ADA and ADC, located at 16 and -19 m along the beam line with respect to the nominal interaction point and covering the pseudorapidity ranges $4.8 < \eta < 6.3$ and $-7.0 < \eta < -4.9$, respectively [22,23].

The ITS is a silicon based detector and is made of six cylindrical layers using three different technologies. The Silicon Pixel Detector (SPD) forms the two innermost layers of the ITS and covers $|\eta| < 2$ and $|\eta| < 1.4$, respectively. Apart from tracking, the SPD is also used for triggering purposes and to reconstruct the primary vertex.

The ITS is cylindrically surrounded by the TPC, whose main purpose is to track particles and provide charged-particle momentum measurements with good two-track separation and particle identification. The TPC coverage in pseudorapidity is $|\eta| < 0.9$ for tracks with full radial length. The TPC has full coverage in azimuth. It offers good momentum resolution in a large range of the track transverse momentum spanning from 0.1 GeV/c to 100 GeV/c.

The TOF is a large cylindrical gaseous detector based on multi-gap resistive-plate chambers. It covers the pseudorapidity region $|\eta| < 0.8$. The TOF readout channels are arranged into 18 azimuthal sectors which can provide topological trigger decisions.

3. Data analysis

3.1. Event selection

The online event selection was based on a dedicated UPC trigger which selected back-to-back tracks in an otherwise empty detector. This selection required (i) that nothing above the trigger threshold was detected in the V0 and AD detectors, (ii) a topological trigger requiring less than eight SPD chips with trigger signal, forming at least two pairs; each pair was required to have an SPD chip fired in each of the two layers and to be in compatible azimuthal sectors, with an opening angle in azimuth between the two pairs larger than 144°, (iii) a topological trigger in the TOF requiring more than one and less than seven TOF sectors to register a signal; at least two of these sectors should have an opening angle in azimuth larger than 150°.

The integrated luminosity of the analysed sample is 233 μb^{-1}. The determination of the luminosity is obtained from the counts of a reference trigger based on multiplicity selection in the V0 detector, with the corresponding cross section estimated from a van der Meer scan; this procedure has an uncertainty of 2.2% [24]. The determination of the live-time of the UPC trigger has an additional uncertainty of 1.5%. The total relative systematic uncertainty of the integrated luminosity is thus 2.7%.

Additional offline V0 and AD veto decisions were applied in the analysis. The offline veto algorithm improved the signal to background ratio, because it utilised a larger timing window to integrate the signal than its online counterpart. Some good events were lost due to this selection. The loss was taken into account with the correction on veto trigger inefficiency discussed in Sec. 3.4. The systematic uncertainty from the V0 and AD vetoes was estimated as the relative change in the measured J/ψ cross section before and after imposing them and correcting for the losses; it amounts to 3%.

Each event had a reconstructed primary vertex within 15 cm from the nominal interaction point along the beam direction, z, and had exactly two tracks. These tracks were reconstructed using combined tracking in the ITS and TPC. Tracks were requested to have at least 70 (out of 159) TPC space points and to have a hit in each of the two layers of the SPD. Each track had to have a distance of closest approach to the event interaction vertex of less than 2 cm in the z-axis direction. Also, each track was required to have $|\eta| < 0.9$. The relative systematic uncertainty from tracking, which takes into account the track quality selection and the track propagation from the TPC to the ITS, was estimated from a comparison of data and Monte Carlo simulation. The combined uncertainty to reconstruct both tracks is 2.8%.

The particle identification (PID) was provided by the specific ionisation losses in the TPC, which offer a large separation power between muons and electrons from the leptonic decays of the J/ψ in the momentum range (1.0, 2.0) GeV/c, relevant for this analysis. The effect of a possible misidentification was found to be negligible.

An offline SPD decision was also applied in the analysis. The offline topological SPD algorithm ensured that the selected tracks crossed the SPD chips used in the trigger decision. The relative systematic uncertainty from the SPD and TOF trigger amounts to 1.3%, which was estimated using a data-driven method by changing the requirements on the probe tracks.

The selected events were required to have tracks with opposite electric charge, the rapidity of the dimuon candidate was restricted to $|y| < 0.8$ and its p_T had to be less than 0.11 GeV/c, in order to obtain a sample dominated by coherent interactions

5 1/2 double-column pages
Two figs, 3 tables. 48 refs.
Five Sections:
- Introduction
- Detector description
- Data analysis
- Results
- Conclusions

Let's look at one paper

Physics Letters B 817 (2021) 136280

Contents lists available at ScienceDirect

Physics Letters B

www.elsevier.com/locate/physletb

First measurement of the $|t|$-dependence of coherent J/ψ photonuclear production

ALICE Collaboration *

ARTICLE INFO

Article history:
Received 24 January 2021
Received in revised form 17 March 2021
Accepted 6 April 2021
Available online 15 April 2021
Editor: M. Doser

ABSTRACT

The first measurement of the cross section for coherent J/ψ photoproduction as a function of $|t|$, the square of the momentum transferred between the incoming and outgoing target nucleus, is presented. The data were measured with the ALICE detector in ultra-peripheral Pb–Pb collisions at a centre-of-mass energy per nucleon pair $\sqrt{s_{\rm NN}} = 5.02$ TeV with the J/ψ produced in the central rapidity region $|y| < 0.8$, which corresponds to the small Bjorken-x range $(0.3 - 1.4) \times 10^{-3}$.
The measured $|t|$-dependence is not described by computations based only on the Pb nuclear form factor, while the photonuclear cross section is better reproduced by models including shadowing according to the leading-twist approximation, or gluon-saturation effects from the impact-parameter dependent Balitsky–Kovchegov equation. These new results are therefore a valid tool to constrain the relevant model parameters and to investigate the transverse gluonic structure at very low Bjorken-x.

1. Introduction

Photonuclear reactions can be studied in ultra-peripheral collisions (UPCs) of heavy ions where the two projectiles pass each other with an impact parameter larger than the sum of their radii. In this case, purely hadronic interactions are suppressed and electromagnetically induced processes occur via photons with typically very small virtualities, of the order of tens of MeV^2. The intensity of the photon flux is proportional to the square of the electric charge of the nuclei, resulting in large cross sections for the coherent photoproduction of a vector meson in UPCs of Pb ions at the LHC. This process has a clear experimental signature: the decay products of the vector meson are the only particles detected in an otherwise empty detector.

The physics of vector meson photoproduction is described, e.g., in Refs. [1–4]. Two vector meson photoproduction processes, coherent and incoherent, are relevant for the results presented here. In the former, the photon interacts with all nucleons in a nucleus, while in the latter it interacts with a single nucleon. In both cases a single vector meson is produced. Experimentally, one can distinguish between these two production types through the transverse momentum $p_{\rm T}$ of the vector meson which is related to the transverse size of the target. While coherent photoproduction is characterised by an average transverse momentum $\langle p_{\rm T}\rangle \sim 60$ MeV/c, incoherent production leads to higher average transverse momenta: $\langle p_{\rm T}\rangle \sim 500$ MeV/c. Incoherent photoproduction can also be accompanied by the excitation and dissociation of the target nucleon resulting in an even higher transverse momentum of the produced vector meson [5].

Shadowing, the observation that the structure of a nucleon inside nuclear matter is different from that of a free nucleon [6], is not yet completely understood and several processes may have a role in different kinematic regions. In this context, coherent heavy vector meson photoproduction is of particular interest, because it is especially sensitive to the gluon distribution in the target, and thus to gluon shadowing effects at low Bjorken-x [7,8]. One of the effects expected to contribute to shadowing in this kinematic region is saturation, a dynamic equilibrium between gluon radiation and recombination [9]. The momentum scale of the interaction (Q^2) is related to the mass m_V of the vector meson as $Q^2 \sim m_V^2/4$, corresponding to the perturbative regime of quantum chromodynamics (QCD) in the case of charmonium states. The rapidity of the coherently produced $c\bar{c}$ states is related to the Bjorken-x of the gluonic exchange as $x = (m_V/\sqrt{s_{\rm NN}})\exp(\pm y)$, where the two signs indicate that either of the incoming ions can be the source of the photon. Thus, the charmonium photoproduction cross section at midrapidity in Pb–Pb UPCs at the LHC Run 2 centre-of-mass energy per nucleon pair of $\sqrt{s_{\rm NN}} = 5.02$ TeV is sensitive to $x \in (0.3, 1.4) \times 10^{-3}$ at ALICE. It thereby provides information on the gluon distribution in nuclei in a kinematic region where shadowing could be present and saturation effects may be important [10,11].

Charmonium photoproduction in ultra-peripheral Pb–Pb collisions was previously studied by the ALICE Collaboration at $\sqrt{s_{\rm NN}} = 2.76$ TeV [12–14]. The coherent J/ψ photoproduction cross section was measured both at midrapidity $|y| < 0.9$ and at forward

* *E-mail address:* alice-publications@cern.ch.

https://doi.org/10.1016/j.physletb.2021.136280

rapidity $-3.6 < y < -2.6$. Recently, a measurement of the rapidity dependence of coherent J/ψ photoproduction at forward rapidity at the higher energy of $\sqrt{s_{\rm NN}} = 5.02$ TeV was also published by the ALICE Collaboration [15]. In addition, the CMS Collaboration studied the coherent J/ψ photoproduction accompanied by neutron emission at semi-forward rapidity $1.8 < |y| < 2.3$ at $\sqrt{s_{\rm NN}} = 2.76$ TeV [16]. These measurements allow for a deeper insight into the rapidity dependence of gluon shadowing, but do not give information on the behaviour of gluons in the impact-parameter plane. The square of the momentum transferred to the target nucleus, $|t|$, is related through a two-dimensional Fourier transform to the gluon distribution in the plane transverse to the interaction [17]; thus the study of the $|t|$-dependence of coherent J/ψ photoproduction provides information about the spatial distribution of gluons as a function of the impact parameter. Thus far, the only measurements in this direction were performed recently by the STAR Collaboration for the case of the ρ^0 vector meson [18] and for the yield of J/ψ in semi-central Au–Au collisions [19].

In this Letter, the first measurement of the $|t|$-dependence of the coherent J/ψ photoproduction cross section at midrapidity in Pb–Pb UPCs at $\sqrt{s_{\rm NN}} = 5.02$ TeV is presented. The J/ψ vector mesons were reconstructed in the rapidity range $|y| < 0.8$ through their decay into $\mu^+\mu^-$, taking advantage of the better mass and momentum resolution of this channel with respect to the e^+e^- channel. The data sample, recorded in 2018, is approximately 10 times larger than that used in previous ALICE measurements at midrapidity at the lower energy of $\sqrt{s_{\rm NN}} = 2.76$ TeV [14]. Cross sections are reported for six $|t|$ intervals and compared with theoretical predictions.

2. Detector description

The ALICE detector and its performance are described in Refs. [20,21]. Three central barrel detectors, the Inner Tracking System (ITS), the Time Projection Chamber (TPC), and the Time-of-Flight (TOF), in addition to two forward detectors, V0 and the ALICE Diffractive (AD) arrays, are used in this analysis. The central barrel detectors are surrounded by a large solenoid magnet producing a magnetic field of $B = 0.5$ T. The V0, AD, ITS, and TOF detectors are used for triggering, the ITS and the TPC for particle tracking, and the TPC for particle identification.

The V0 is a scintillator detector made of two counters, V0A and V0C, installed on both sides of the interaction point. The V0A and V0C cover the pseudorapidity ranges $2.8 < \eta < 5.1$ and $-3.7 < \eta < -1.7$, respectively. Both counters are segmented in four rings in the radial direction, with each ring divided into 8 sections in azimuth.

The AD consists of two scintillator stations, ADA and ADC, located at 16 and -19 m along the beam line with respect to the nominal interaction point and covering the pseudorapidity ranges $4.8 < \eta < 6.3$ and $-7.0 < \eta < -4.9$, respectively [22,23].

The ITS is a silicon based detector and is made of six cylindrical layers using three different technologies. The Silicon Pixel Detector (SPD) forms the two innermost layers of the ITS and covers $|\eta| < 2$ and $|\eta| < 1.4$, respectively. Apart from tracking, the SPD is also used for triggering purposes and to reconstruct the primary vertex.

The ITS is cylindrically surrounded by the TPC, whose main purpose is to track particles and provide charged-particle momentum measurements with good two-track separation and particle identification. The TPC coverage in pseudorapidity is $|\eta| < 0.9$ for tracks with full radial length. The TPC has full coverage in azimuth. It offers good momentum resolution in a large range of the track transverse momentum spanning from 0.1 GeV/c to 100 GeV/c.

The TOF is a large cylindrical gaseous detector based on multi-gap resistive-plate chambers. It covers the pseudorapidity region $|\eta| < 0.8$. The TOF readout channels are arranged into 18 azimuthal sectors which can provide topological trigger decisions.

3. Data analysis

3.1. Event selection

The online event selection was based on a dedicated UPC trigger which selected back-to-back tracks in an otherwise empty detector. This selection required (i) that nothing above the trigger threshold was detected in the V0 and AD detectors, (ii) a topological trigger requiring less than eight SPD chips with trigger signal, forming at least two pairs; each pair was required to have an SPD chip fired in each of the two layers and to be in compatible azimuthal sectors, with an opening angle in azimuth between the two pairs larger than 144°, (iii) a topological trigger in the TOF requiring more than one and less than seven TOF sectors to register a signal; at least two of these sectors should have an opening angle in azimuth larger than 150°.

The integrated luminosity of the analysed sample is 233 μb^{-1}. The determination of the luminosity is obtained from the counts of a reference trigger based on multiplicity selection in the V0 detector, with the corresponding cross section estimated from a van der Meer scan; this procedure has an uncertainty of 2.2% [24]. The determination of the live-time of the UPC trigger has an additional uncertainty of 1.5%. The total relative systematic uncertainty of the integrated luminosity is thus 2.7%.

Additional offline V0 and AD veto decisions were applied in the analysis. The offline veto algorithm improved the signal to background ratio, because it utilised a larger timing window to integrate the signal than its online counterpart. Some good events were lost due to this selection. The loss was taken into account with the correction on veto trigger inefficiency discussed in Sec. 3.4. The systematic uncertainty from the V0 and AD vetoes was estimated as the relative change in the measured J/ψ cross section before and after imposing them and correcting for the losses; it amounts to 3%.

Each event had a reconstructed primary vertex within 15 cm from the nominal interaction point along the beam direction, z, and had exactly two tracks. These tracks were reconstructed using combined tracking in the ITS and TPC. Tracks were requested to have at least 70 (out of 159) TPC space points and to have a hit in each of the two layers of the SPD. Each track had to have a distance of closest approach to the event interaction vertex of less than 2 cm in the z-axis direction. Also, each track was required to have $|\eta| < 0.9$. The relative systematic uncertainty from tracking, which takes into account the track quality selection and the track propagation from the TPC to the ITS, was estimated from a comparison of data and Monte Carlo simulation. The combined uncertainty to reconstruct both tracks is 2.8%.

The particle identification (PID) was provided by the specific ionisation losses in the TPC, which offer a large separation power between muons and electrons from the leptonic decays of the J/ψ in the momentum range (1.0, 2.0) GeV/c, relevant for this analysis. The effect of a possible misidentification was found to be negligible.

An offline SPD decision was also applied in the analysis. The offline topological SPD algorithm ensured that the selected tracks crossed the SPD chips used in the trigger decision. The relative systematic uncertainty from the SPD and TOF trigger amounts to 1.3%, which was estimated using a data-driven method by changing the requirements on the probe tracks.

The selected events were required to have tracks with opposite electric charge, the rapidity of the dimuon candidate was restricted to $|y| < 0.8$ and its $p_{\rm T}$ had to be less than 0.11 GeV/c, in order to obtain a sample dominated by coherent interactions

5 1/2 double-column pages
Two figs, 3 tables. 48 refs.
Five Sections:
- Introduction
- Detector description
- Data analysis
- Results
- Conclusions

Introduction: 5 paragraphs

1. Introduction

Photonuclear reactions can be studied in ultra-peripheral collisions (UPCs) of heavy ions where the two projectiles pass each other with an impact parameter larger than the sum of their radii. In this case, purely hadronic interactions are suppressed and electromagnetically induced processes occur via photons with typically very small virtualities, of the order of tens of MeV^2. The intensity of the photon flux is proportional to the square of the electric charge of the nuclei, resulting in large cross sections for the coherent photoproduction of a vector meson in UPCs of Pb ions at the LHC. This process has a clear experimental signature: the decay products of the vector meson are the only particles detected in an otherwise empty detector.

UPC definition

The physics of vector meson photoproduction is described, e.g., in Refs. [1–4]. Two vector meson photoproduction processes, coherent and incoherent, are relevant for the results presented here. In the former, the photon interacts with all nucleons in a nucleus, while in the latter it interacts with a single nucleon. In both cases a single vector meson is produced. Experimentally, one can distinguish between these two production types through the transverse momentum p_{T} of the vector meson which is related to the transverse size of the target. While coherent photoproduction is characterised by an average transverse momentum $\langle p_{\mathrm{T}} \rangle \sim 60$ MeV/c, incoherent production leads to higher average transverse momenta: $\langle p_{\mathrm{T}} \rangle \sim 500$ MeV/c. Incoherent photoproduction can also be accompanied by the excitation and dissociation of

Let's look at the Introduction (1/3)

1. Introduction

Photonuclear reactions can be studied in ultra-peripheral collisions (UPCs) of heavy ions where the two projectiles pass each other with an impact parameter larger than the sum of their radii. In this case, purely hadronic interactions are suppressed and electromagnetically induced processes occur via photons with typically very small virtualities, of the order of tens of MeV^2. The intensity of the photon flux is proportional to the square of the electric charge of the nuclei, resulting in large cross sections for the coherent photoproduction of a vector meson in UPCs of Pb ions at the LHC. This process has a clear experimental signature: the decay products of the vector meson are the only particles detected in an otherwise empty detector.

UPC definition

Why: pure hadronic interactions are suppressed and photonuclear interactions are not

The physics of vector meson photoproduction is described, e.g., in Refs. [1–4]. Two vector meson photoproduction processes, coherent and incoherent, are relevant for the results presented here. In the former, the photon interacts with all nucleons in a nucleus, while in the latter it interacts with a single nucleon. In both cases a single vector meson is produced. Experimentally, one can distinguish between these two production types through the transverse momentum p_T of the vector meson which is related to the transverse size of the target. While coherent photoproduction is characterised by an average transverse momentum $\langle p_T \rangle \sim 60$ MeV/c, incoherent production leads to higher average transverse momenta: $\langle p_T \rangle \sim 500$ MeV/c. Incoherent photoproduction can also be accompanied by the excitation and dissociation of

Let's look at the Introduction (1/3)

1. Introduction

Photonuclear reactions can be studied in ultra-peripheral collisions (UPCs) of heavy ions where the two projectiles pass each other with an impact parameter larger than the sum of their radii. In this case, purely hadronic interactions are suppressed and electromagnetically induced processes occur via photons with typically very small virtualities, of the order of tens of MeV^2. The intensity of the photon flux is proportional to the square of the electric charge of the nuclei, resulting in large cross sections for the coherent photoproduction of a vector meson in UPCs of Pb ions at the LHC. This process has a clear experimental signature: the decay products of the vector meson are the only particles detected in an otherwise empty detector.

UPC definition

Why: pure hadronic interactions are suppressed and photonuclear interactions are not

Not only a nice idea, but also a feasible one

The physics of vector meson photoproduction is described, e.g., in Refs. [1–4]. Two vector meson photoproduction processes, coherent and incoherent, are relevant for the results presented here. In the former, the photon interacts with all nucleons in a nucleus, while in the latter it interacts with a single nucleon. In both cases a single vector meson is produced. Experimentally, one can distinguish between these two production types through the transverse momentum p_{T} of the vector meson which is related to the transverse size of the target. While coherent photoproduction is characterised by an average transverse momentum $\langle p_{\mathrm{T}} \rangle \sim 60$ MeV/c, incoherent production leads to higher average transverse momenta: $\langle p_{\mathrm{T}} \rangle \sim 500$ MeV/c. Incoherent photoproduction can also be accompanied by the excitation and dissociation of

Let's look at the Introduction (1/3)

1. Introduction

Photonuclear reactions can be studied in ultra-peripheral collisions (UPCs) of heavy ions where the two projectiles pass each other with an impact parameter larger than the sum of their radii. In this case, purely hadronic interactions are suppressed and electromagnetically induced processes occur via photons with typically very small virtualities, of the order of tens of MeV^2. The intensity of the photon flux is proportional to the square of the electric charge of the nuclei, resulting in large cross sections for the coherent photoproduction of a vector meson in UPCs of Pb ions at the LHC. This process has a clear experimental signature: the decay products of the vector meson are the only particles detected in an otherwise empty detector.

The physics of vector meson photoproduction is described, e.g., in Refs. [1–4]. Two vector meson photoproduction processes, coherent and incoherent, are relevant for the results presented here. In the former, the photon interacts with all nucleons in a nucleus, while in the latter it interacts with a single nucleon. In both cases a single vector meson is produced. Experimentally, one can distinguish between these two production types through the transverse momentum p_{T} of the vector meson which is related to the transverse size of the target. While coherent photoproduction is characterised by an average transverse momentum $\langle p_{\mathrm{T}} \rangle \sim 60$ MeV/c, incoherent production leads to higher average transverse momenta: $\langle p_{\mathrm{T}} \rangle \sim 500$ MeV/c. Incoherent photoproduction can also be accompanied by the excitation and dissociation of

12 lines, 4 sentences, one paragraph

UPC definition

Why: pure hadronic interactions are suppressed and photonuclear interactions are not

Not only a nice idea, but also a feasible one

Let's look at the Introduction (1/3)

1. Introduction

Photonuclear reactions can be studied in ultra-peripheral collisions (UPCs) of heavy ions where the two projectiles pass each other with an impact parameter larger than the sum of their radii. In this case, purely hadronic interactions are suppressed and electromagnetically induced processes occur via photons with typically very small virtualities, of the order of tens of MeV^2. The intensity of the photon flux is proportional to the square of the electric charge of the nuclei, resulting in large cross sections for the coherent photoproduction of a vector meson in UPCs of Pb ions at the LHC. This process has a clear experimental signature: the decay products of the vector meson are the only particles detected in an otherwise empty detector.

The physics of vector meson photoproduction is described, e.g., in Refs. [1–4]. Two vector meson photoproduction processes, coherent and incoherent, are relevant for the results presented here. In the former, the photon interacts with all nucleons in a nucleus, while in the latter it interacts with a single nucleon. In both cases a single vector meson is produced. Experimentally, one can distinguish between these two production types through the transverse momentum p_{T} of the vector meson which is related to the transverse size of the target. While coherent photoproduction is characterised by an average transverse momentum $\langle p_{\mathrm{T}} \rangle \sim 60$ MeV/c, incoherent production leads to higher average transverse momenta: $\langle p_{\mathrm{T}} \rangle \sim 500$ MeV/c. Incoherent photoproduction can also be accompanied by the excitation and dissociation of

12 lines, 4 sentences, one paragraph

UPC definition

Why: pure hadronic interactions are suppressed and photonuclear interactions are not

Not only a nice idea, but also a feasible one

Refer to a review, introduce nomenclature

1. Introduction

Photonuclear reactions can be studied in ultra-peripheral collisions (UPCs) of heavy ions where the two projectiles pass each other with an impact parameter larger than the sum of their radii. In this case, purely hadronic interactions are suppressed and electromagnetically induced processes occur via photons with typically very small virtualities, of the order of tens of MeV^2. The intensity of the photon flux is proportional to the square of the electric charge of the nuclei, resulting in large cross sections for the coherent photoproduction of a vector meson in UPCs of Pb ions at the LHC. This process has a clear experimental signature: the decay products of the vector meson are the only particles detected in an otherwise empty detector.

The physics of vector meson photoproduction is described, e.g., in Refs. [1–4]. Two vector meson photoproduction processes, coherent and incoherent, are relevant for the results presented here. In the former, the photon interacts with all nucleons in a nucleus, while in the latter it interacts with a single nucleon. In both cases a single vector meson is produced. Experimentally, one can distinguish between these two production types through the transverse momentum p_{T} of the vector meson which is related to the transverse size of the target. While coherent photoproduction is characterised by an average transverse momentum $\langle p_{\mathrm{T}} \rangle \sim 60$ MeV/c, incoherent production leads to higher average transverse momenta: $\langle p_{\mathrm{T}} \rangle \sim 500$ MeV/c. Incoherent photoproduction can also be accompanied by the excitation and dissociation of

12 lines, 4 sentences, one paragraph

UPC definition

Why: pure hadronic interactions are suppressed and photonuclear interactions are not

Not only a nice idea, but also a feasible one

Refer to a review, introduce nomenclature

How you use the physics characteristics of the processes to distinguish them experimentally

Let's look at the Introduction (2/3)

the target nucleon resulting in an even higher transverse momentum of the produced vector meson [5].

Shadowing, the observation that the structure of a nucleon inside nuclear matter is different from that of a free nucleon [6], is not yet completely understood and several processes may have a role in different kinematic regions. In this context, coherent heavy vector meson photoproduction is of particular interest, because it is especially sensitive to the gluon distribution in the target, and thus to gluon shadowing effects at low Bjorken-x [7,8]. One of the effects expected to contribute to shadowing in this kinematic region is saturation, a dynamic equilibrium between gluon radiation and recombination [9]. The momentum scale of the interaction (Q^2) is related to the mass m_V of the vector meson as $Q^2 \sim m_V^2/4$, corresponding to the perturbative regime of quantum chromodynamics (QCD) in the case of charmonium states. The rapidity of the coherently produced $c\bar{c}$ states is related to the Bjorken-x of the gluonic exchange as $x = \left(m_V/\sqrt{s_{\mathrm{NN}}}\right)\exp(\pm y)$, where the two signs indicate that either of the incoming ions can be the source of the photon. Thus, the charmonium photoproduction cross section at midrapidity in Pb–Pb UPCs at the LHC Run 2 centre-of-mass energy per nucleon pair of $\sqrt{s_{\mathrm{NN}}} = 5.02$ TeV is sensitive to $x \in (0.3, 1.4) \times 10^{-3}$ at ALICE. It thereby provides information on the gluon distribution in nuclei in a kinematic region where shadowing could be present and saturation effects may be important [10,11].

Charmonium photoproduction in ultra-peripheral Pb–Pb collisions was previously studied by the ALICE Collaboration at $\sqrt{s_{\mathrm{NN}}} = 2.76$ TeV [12–14]. The coherent J/ψ photoproduction cross section was measured both at midrapidity $|y| < 0.9$ and at forward

what is the physics we are interested in and how it relates to this work

What new ingredient is contributed by this measurement?

What has been done before in this area?

Let's look at the Introduction (3/3)

rapidity $-3.6 < y < -2.6$. Recently, a measurement of the rapidity dependence of coherent J/ψ photoproduction at forward rapidity at the higher energy of $\sqrt{s_{\mathrm{NN}}} = 5.02$ TeV was also published by the ALICE Collaboration [15]. In addition, the CMS Collaboration studied the coherent J/ψ photoproduction accompanied by neutron emission at semi-forward rapidity $1.8 < |y| < 2.3$ at $\sqrt{s_{\mathrm{NN}}} = 2.76$ TeV [16]. These measurements allow for a deeper insight into the rapidity dependence of gluon shadowing, but do not give information on the behaviour of gluons in the impact-parameter plane. The square of the momentum transferred to the target nucleus, $|t|$, is related through a two-dimensional Fourier transform to the gluon distribution in the plane transverse to the interaction [17]; thus the study of the $|t|$-dependence of coherent J/ψ photoproduction provides information about the spatial distribution of gluons as a function of the impact parameter. Thus far, the only measurements in this direction were performed recently by the STAR Collaboration for the case of the ρ^0 vector meson [18] and for the yield of J/ψ in semi-central Au–Au collisions [19].

What has been done before in this area?

In this Letter, the first measurement of the $|t|$-dependence of the coherent J/ψ photoproduction cross section at midrapidity in Pb–Pb UPCs at $\sqrt{s_{\mathrm{NN}}} = 5.02$ TeV is presented. The J/ψ vector mesons were reconstructed in the rapidity range $|y| < 0.8$ through their decay into $\mu^+\mu^-$, taking advantage of the better mass and momentum resolution of this channel with respect to the e^+e^- channel. The data sample, recorded in 2018, is approximately 10 times larger than that used in previous ALICE measurements at midrapidity at the lower energy of $\sqrt{s_{\mathrm{NN}}} = 2.76$ TeV [14]. Cross sections are reported for six $|t|$ intervals and compared with theoretical predictions.

What do we do in this work

Random closing comments

If you are familiar with a topic and know what was done and why, then a structure for an article and for each of its sections should come naturally to you ... do not try to invent a sophisticated way of telling the story ... straight language without any extra spice should be enough ....

Random closing comments

If you do not know why, ASK!!!

If you are familiar with a topic and know what was done and why, then a structure for an article and for each of its sections should come naturally to you ... do not try to invent a sophisticated way of telling the story ... straight language without any extra spice should be enough ....

Random closing comments

If you do not know why, ASK!!!

If you are familiar with a topic and know what was done and why, then a structure for an article and for each of its sections should come naturally to you ... do not try to invent a sophisticated way of telling the story ... straight language without any extra spice should be enough ....

The same advice of thinking the structure before writing and of counting applies to preparing slides for a talk ...

Random closing comments

If you do not know why, ASK!!!

If you are familiar with a topic and know what was done and why, then a structure for an article and for each of its sections should come naturally to you ... do not try to invent a sophisticated way of telling the story ... straight language without any extra spice should be enough ....

The same advice of thinking the structure before writing and of counting applies to preparing slides for a talk ...

The new ingredient is the time to say aloud one normal sentence ... allow for 10 s, meaning you have 6 nice long sentences to describe one slide :)

Random closing comments

If you do not know why, ASK!!!

If you are familiar with a topic and know what was done and why, then a structure for an article and for each of its sections should come naturally to you ... do not try to invent a sophisticated way of telling the story ... straight language without any extra spice should be enough ....

The same advice of thinking the structure before writing and of counting applies to preparing slides for a talk ...

The new ingredient is the time to say aloud one normal sentence ... allow for 10 s, meaning you have 6 nice long sentences to describe one slide :)

If you do not have a clear idea of a potential structure for the text, then you may not have understood well what you did, or why you did it ... go for a walk (or whatever) and think a bit before putting pen to paper :)

Random closing comments

If you do not know why, ASK!!!

If you are familiar with a topic and know what was done and why, then a structure for an article and for each of its sections should come naturally to you ... do not try to invent a sophisticated way of telling the story ... straight language without any extra spice should be enough ....

The same advice of thinking the structure before writing and of counting applies to preparing slides for a talk ...

The new ingredient is the time to say aloud one normal sentence ... allow for 10 s, meaning you have 6 nice long sentences to describe one slide :)

If you do not have a clear idea of a potential structure for the text, then you may not have understood well what you did, or why you did it ... go for a walk (or whatever) and think a bit before putting pen to paper :)

Read papers. If there is one that you like, try to find out why you like it, and dissect it ... i.e. learn from the masters